AKADÉMIAI KIADÓ

Uridine alleviates LPS-induced ARDS and improves insulin sensitivity by decreasing oxidative stress and inflammatory processes

LEI ZHANG[1], BIN LI[1], DEGANG ZHANG[2], ZHUO WANG[3], YE ZHAO[1] and QIN YU[1]*

[1] Department of Critical Care Medicine, The First Hospital of Lanzhou University, The First School of Clinical Medicine of Lanzhou University, Lanzhou City 730000, Gansu, China

[2] Department of Respiratory Medicine, Lanzhou University Second Hospital, Lanzhou City 730000, China

[3] Department of Pathology, Gansu Provincial Hospital, Lanzhou City 730050, Gansu, China

Check for updates

ABSTRACT

Acute respiratory distress syndrome (ARDS) refers to the injury of alveolar epithelial cells and capillary endothelial cells due to various injury factors. Research on the pathogenesis of ARDS has made great progress, but the exact pathogenesis of ARDS has not been fully elucidated. Up to now, the prevention and treatment of ARDS is still an important scientific problem that needs to be solved urgently. In this work, we analyzed the effect of uridine on ARDS. An ARDS model was successfully constructed by lipopolysaccharide (LPS) stimulation. Western-blotting, IFA, ELISA, RT-PCT and CLSM were conducted to investigate the effect of uridine on ARDS and insulin resistance, and the results showed that lung histopathological alterations were significantly attenuated by uridine treatment. Further work showed that the levels of proinflammatory cytokines were significantly down-regulated in the lung tissue after treatment with uridine. Additionally, the numbers of total cells and neutrophils in the bronchoalveolar lavage fluid (BALF) were also decreased in the uridine-treated ARDS mice. We further explored the potential mechanism by which uridine could treat ARDS, and the results indicated that NF-κB signaling was down-regulated by uridine treatment. Next, we studied insulin sensitivity in the ARDS mice, and found that insulin signaling was significantly down-regulated, and uridine could enhance insulin sensitivity in the ARDS mice model. Furthermore, we found that the levels of inflammation and oxidative stress were

* Corresponding author. Department of Critical Care Medicine, The First Hospital of Lanzhou University, Lanzhou City, 1 Donggang West Rd, Chengguan district, Lanzhou, Gansu province, Lanzhou, Gansu, 730000, China. Tel.: +86 0931-8281114. E-mail: yuqin@lzu.edu.cn

AKJournals

decreased by uridine treatment, which may be the potential mechanism by which uridine could improve insulin sensitivity. Taken together, the current work provides evidence that uridine can serve as a potential drug to treat ARDS and insulin resistance.

INTRODUCTION

Acute respiratory distress syndrome (ARDS) refers to the damage of alveolar epithelial cells and capillary endothelial cells induced by various physical and chemical damage factors, which result in progressive dyspnea and refractory hypoxemia [1–3]. ARDS is one of the main causes of death in ICU (intensive care unit) patients [4, 5]. ARDS is characterized by severe lung inflammation, causing the destruction of the pulmonary microvascular endothelial barrier [4]. These pathological factors impair the lung's gas exchange and alveolar surface function, and the patient develops severe hypoxemia and elevated pulmonary artery wedge pressure. The etiology of ARDS is very complicated. After half a century, research on the pathogenesis of ARDS has made great progress, but the exact pathogenesis of ARDS has not been fully elucidated [6]. It is generally believed that the excessive activation and recruitment of inflammatory cells in the lung, the activation of a large number of inflammatory factors and effector cells, and the uncontrolled inflammatory response caused by ARDS are the main pathophysiological changes in ARDS [2, 3]. Therefore, inhibition of uncontrolled inflammation may be a way to treat ARDS. A series of studies have shown that the use of biologically active molecules could treat ARDS. It has been reported that Astilbin could alleviate LPS-induced ARDS through inhibiting MAPK (Mitogen-activated protein kinase) signaling [7].

Studies have reported that, in addition to causing significant damage to the lungs, ARDS also has important effects on other organs. ARDS may seriously affect the endocrine system [8–10]. However, until now, the potential impact of ARDS on insulin sensitivity remains unclear.

Uridine is a pyrimidine nucleoside that consists of uracil and ribose and is a constituent of RNA in all living organisms. A series of studies have shown that uridine has important biological activities, such as treatment of inflammation and regulation of nerve function [11]. In the current research, an *in vivo* and *in vitro* ARDS model was established. On this basis we explored the effect of uridine on ARDS, and found that uridine could alleviate the lung damage caused by ARDS. In addition, the experimental results showed that ARDS led to insulin resistance, however uridine treatment could enhance insulin sensitivity in the ARDS model. In short, the current research indicates that uridine showed therapeutic potential for ARDS. Furthermore, uridine could also alleviate insulin resistance caused by ARDS. Taken together, the current work provides preclinical evidence that uridine can serve as a potential therapeutic drug to treat ARDS.

MATERIALS AND METHODS

Reagents

Insulin, lipopolysaccharide (LPS), and bovine serum albumin (BSA) were obtained from Sigma Aldrich (USA). Streptomycin and penicillin were purchased from Beyotime (Shanghai, China).

The 3-(4,5-dimethylthiazol-2-yl)-2,5-diphenyltetrazolium (MTT) assay kit (Cat No: C0009S) was obtained from Beyotime Biotechnology (Shanghai, China). HRP-conjugated secondary antibody was from Abcam (Cambridge, UK). Tubulin (Cat No: A17913) and β-actin (Cat No: AC038) antibodies were obtained from ABclonal Biotechnology Co., Ltd (China). Anti-p-IκB (Cat No: ab133462, 1:1000 dilution), Anti-JNK (Cat No: ab1993801:1000), Anti-p38 (Cat No: ab31828, 1:500 dilution), and NF-κB (Cat No:ab220803, 1:1000 dilution) were purchased from Abcam (Cambridge, UK). The Superoxide Dismutase (SOD) Activity assay kit (Cat no: BC0170-50T/24) was obtained from Beijing Solarbio Science & Technology Co., Ltd (Beijing China). The Micro Malondialdehyde (MDA) assay kit (Cat no: BC0025-100T/96S) was purchased from Beijing Solarbio Science & Technology Co., Ltd (Beijing, China). The activity of myeloperoxidase (MPO) was analyzed by the MPO Activity assay kit (Cat no:ab105136, Abcam). The Mouse TNF-α ELISA kit (Cat No: SEKM-0034) and the mouse IL-6 ELISA kit (Cat No: SEKM-0007) were purchased from Beijing Solarbio Science & Technology Co., Ltd (Beijing, China). Anti-albumin antibody (Cat No: ab207327) and anti-thrombomodulin antibody (Cat No: ab230010) were purchased from Abcam (Cambridge, UK).

Cell culture

MLE-12 cell (mouse lung epithelial cell line) was purchased from the China Cell Line Bank. The cells were cultured in Dulbecco's modified eagle medium (DMEM) containing 10% fetal bovine serum (FBS) (HyClone), 100 U/mL of penicillin, and 100 U/mL of streptomycin at 37°C.

Animals

All animal procedures were approved by the Animal Care and Use Committee of the first hospital of Lanzhou University (2020–0007). C57BL/6J mice (male), weighing 18–20 g and 6–8 weeks old, were obtained from Beijing Huafukang Biological Technology Co. Ltd (Beijing, China). All animals were housed in clear plastic cages (40 × 30 × 20 cm) at 22 ± 1°C. All animals were maintained on a 12-h light/dark cycle with ~50% humidity. Food and water were supplied ad libitum.

Establishment of ARDS model (*in vivo*)

All experimental animals (C57/BL mice) were randomly allocated into 3 groups ($n = 8$ per group): Control group, LPS group (10 mg kg^{-1}) and LPS plus uridine group (20 mg kg^{-1}). The LPS plus uridine group (20 mg kg^{-1}) was pre-treated with uridine for 24 h, and the control group and the LPS group were pre-treated with an equal volume of vehicle, after which the LPS-treated group and the LPS plus uridine group were treated with LPS (10 mg kg^{-1}). The control group was treated with saline. Insulin sensitivity was assessed by injecting insulin through the tail vein. Lung and liver tissue samples and serum samples were collected for further analyses.

Cell viability assay

MTT analysis was used to evaluate cell viability. MLE-12 cells were plated onto 96-well plates (5 × 10^4 cells/mL). Cells were challenged with different concentrations of uridine for 24 h. After uridine treatment, the cells were treated by LPS (1 μg mL^{-1}), after which 20 μL MTT (4 mg mL^{-1}) was added to each well. After incubation for 4 h at 37°C, the optical density of the cell samples was detected by a microtiter plate reader (Bio-rad).

BALF collection and ELISA assays

12–24 h after LPS stimulation, BALF samples were collected from all mice. The samples were centrifuged (4°C, 4000 rpm, 30 min) to pellet the cells. The inflammatory cytokines in BALF were determined by ELISA kit according to the manufacturer's instructions.

Analysis of serum samples by ELISA

Blood samples were collected after LPS injection during organ harvest. The collected serum samples were analyzed by ELISA according to the manufacturer's instructions.

Western blot analysis

Proteins were extracted from tissues and cells. The concentrations of protein samples were determined by the BCA protein assay kit. Equal amounts of protein sample (30 μg) were separated by 10% SDS-PAGE, after which cell protein samples were transferred onto PVDF membranes. After washing, the membranes were incubated in 5% skim milk at 37°C for 120 min. After washing with TBS-T, the membranes were incubated with primary antibodies (Anti-p-IκB, 1:1000 dilution; Anti-JNK, 1:1000; Anti-p38, 1:500 dilution; NF-κB, 1:1000 dilution) overnight at 4°C. After incubation, the membranes were washed thrice, followed by incubating with secondary antibody (1:3000 dilution) for 60 min on the shaker at RT. After washing for three times, immunoreactive protein bands were detected using enhanced chemiluminescence (ECL). β-actin was used as internal control.

Immunofluorescence (IF) analysis

Cells were seeded onto 6-well glass slides (1.5×10^4 cells/well). After culture for 10 h, the cells were fixed with 4% paraformaldehyde (PFA) at RT for 15 min. After washing, the cells were incubated with 1% Triton X-100 for 0.5 h, and blocked with 5% BSA for 60 min at RT. After three washes, the slides were incubated with the indicated antibodies (SDC-1 (syndecan-1): 1:500 dilution; TNFα: 1:300) at 4°C for 12 h. After washing, the cells were treated with Alexa-488-conjugated secondary antibodies for 120 min at 37°C. DAPI was then used to stain the cells for another 5 min. Cell samples were examined in a fluorescence microscope (Olympus FV1000).

Detection of MPO, MDA, SOD

The activity of SOD was determined by the Superoxide Dismutase (SOD) activity assay kit according to the manufacturer's instruction; MDA concentrations were tested by the Micro Malondialdehyde (MDA) assay kit according to manufacturer's instructions; the activity of myeloperoxidase (MPO) was analyzed by the MPO Activity assay kit according to the manufacturer's instructions.

RT-PCR analysis

Total RNA was extracted using Trizol reagent (Invitrogen). Two μg of the extracted total RNA was used for cDNA synthesis using the RevertAid First Strand cDNA Synthesis kit (Thermo Fisher, Cat no: K1622) following the manufacturer's instructions. RT-PCR was then performed. The following primers were used: IL-1β: Fwd: CAACCAACAAGTGATATTCTCCATG, Rev

GATCCACACTCTCCAGCTGCA; TNFα: Fwd. CATCTTCTCAAAATTCGAGTGACAA, Rev TGGGAGTAGACAAGGTACAACCC; IL-6: Fwd GAGGATACCACTCCCAACAGACC, Rev: AAGTGCATCATCGTTGTTCATACA; The optimal reaction program was the following: 35 cycles of 95°C for 2 min, 94 °C for 45 s, 58 °C for 30 s, 72 °C for 30 s; 72 °C for 5 min. GADPH/β-actin was used as an internal reference. Relative expression level was computed using the $2^{-\Delta\Delta Ct}$ method.

Immunohistochemistry (IHC) analysis

The tissue samples were immersed in 20% neutral buffered formalin, fixed overnight and embedded in paraffin according to standard procedures. The tissue samples were cut into 5-mm-thick sections. Paraffin-embedded lung/liver tissue sections were stained with hematoxylin and eosin (H&E) for histopathological analysis. Lung tissues were analyzed by immunohistochemistry as described previously [12]. In brief, the lung tissues were fixed in 4% PFA in 0.1 M phosphate buffer (pH 7.2), and then embedded in paraffin. Paraffin-embedded lung sections were rehydrated and treated with hydrogen peroxide. After washing for three times, the liver sections were blocked with 5% serum for 2 h at room temperature. After washing, the tissue samples were incubated with primary antibodies, followed by incubation of secondary antibodies for 90 min at RT. After washing the tissue samples, the lung/liver tissue sections were studied in a microscope.

Flow cytometry analysis

After treatment with uridine, the cells were digested and collected. The single-cell suspension was fixed in 70% cold ethanol at 4°C for 24 h. After washing twice with PBS, the concentration of cells was adjusted to 1×10^6/mL. Cells were blocked with BSA for 2 h at room temperature (RT), then incubated with the indicated primary antibodies. After washing twice, fluorescently labeled secondary antibody was added to stain cells, and incubated for 1 h in the dark at RT. After washing for three times, cell samples were analyzed by flow cytometry (BD Accuri C6). DCFH-DA (as a fluorescent probe) was used to detect the ROS level. After treatment the cells were incubated with DCFH-DA (10 μm mL^{-1}) at 37°C for 20 min. After incubation, the cells were washed 3 times, then trypsinized in 0.25% EDTA, and collected by centrifugation. After washing three times with PBS, the fluorescence intensity of each group was measured by flow cytometry (BD Accuri C6).

Statistical analysis

All data are presented as mean $\pm$ SD. Data were assessed using Student's t-test and one-way ANOVA. The statistical significance of differences between the groups was evaluated using a Post Hoc analysis with the Turkey multiple comparison test. The p values were calculated using one-way analysis of variance (ANOVA) with Tukey's post hoc multiple comparison test. $P < 0.05$ was considered statistically significant.

RESULTS

Establishment of ARDS model by LPS treatment

We firstly confirmed whether the ARDS model was successfully established by LPS treatment. After intratracheal instillation with LPS (10 mg kg^{-1}) or vehicle for 24 h, the mice developed

ARDS. As shown in Fig. 1A, pathologic alterations in lung injury (such as inflammatory cells infiltration) could be obviously observed. The levels of TNF-α and IL-6 (proinflammatory cytokines) were determined, and the results indicated that TNF-α and IL-6 were significantly increased in the lung tissue from ARDS mice (Fig. 1B). Additionally, the total numbers of cells and neutrophils in BALF were obviously enhanced (Fig. 1C).
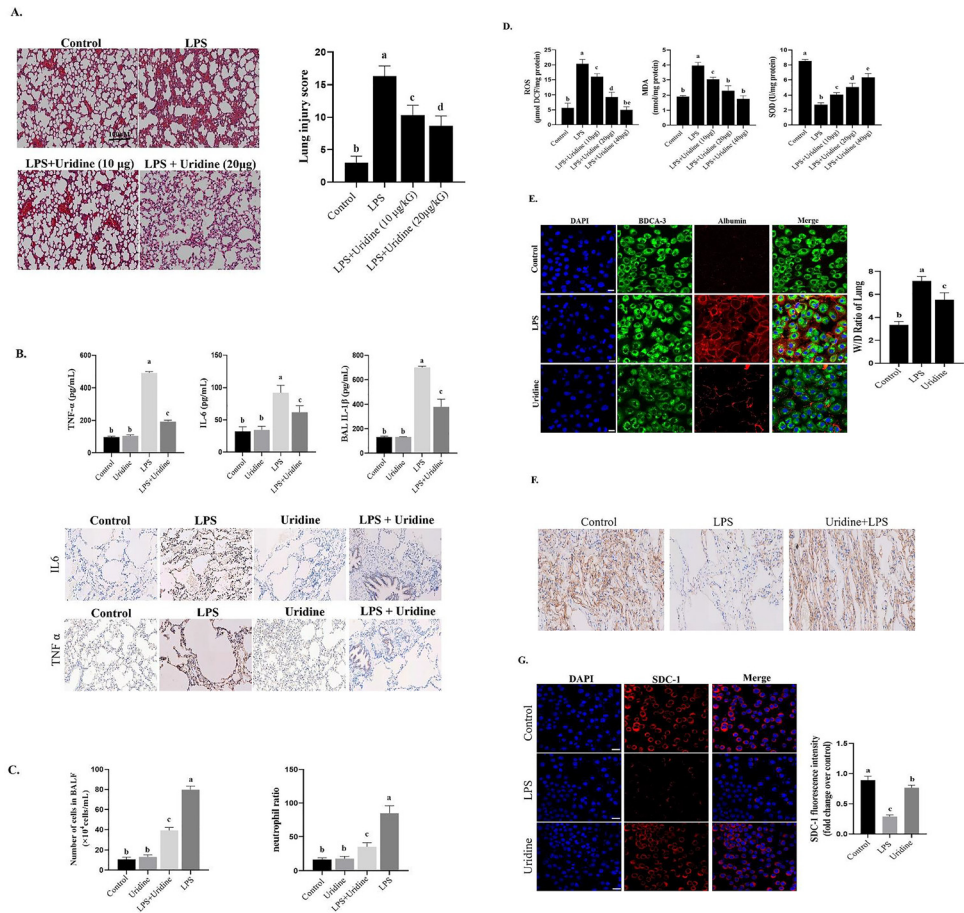

Fig. 1. Effects of uridine on the pathological changes in the lung tissue of ARDS mice
The mice were intragastrically administered with 10 and 20 mg kg^{-1} uridine for 10 consecutive days, after which they were intraperitoneally treated with 10 mg kg^{-1} LPS. A. After 12 h, the lung tissues were collected and assessed by H&E staining (magnification × 200, scale bar = 100 μm); B. Effects of uridine on the levels of pro-inflammatory factors. The concentrations of IL-6/TNF-α/IL-1β were evaluated using commercial ELISA kits. C. The numbers of total cells and neutrophils in the bronchoalveolar lavage fluid (BALF) of ARDS mice were decreased after uridine treatment. D. Effect of uridine on ROS production, MDA and SOD concentration in lung tissue of LPS-induced ARDS mice. E. The effects of uridine on pulmonary vascular permeability in LPS-induced ARDS mice. W/D ratio: Wet-to-dry weight ratio of lung. F. Uridine treatment regulated CD31 expression. G. Uridine inhibited SDC-1 down-regulation. Data are presented as mean ± SD. Different letters indicate significant differences ($P < 0.05$).

At same time, we also analyzed the effects of uridine on LPS-induced ARDS. We can see that LPS-induced histopathological alterations were obviously relieved by uridine treatment (Fig. 1A). The levels of proinflammatory cytokines were also evaluated, and it was found that TNF-α and IL-6 were significantly down-regulated in the lung tissue from ARDS mice after treatment with uridine (Fig. 1B). Additionally, the numbers of total cells and neutrophils in BALF were decreased in the uridine-treated ARDS mice (Fig. 1C). Furthermore, the oxidative stress level (such as MPO and MDA) in the lung tissue was significantly decreased in the uridine-treated group (Fig. 1D). In conclusion, uridine could decrease lung injury and inflammation in ARDS mice.

In addition, we also studied the effects of uridine on Pulmonary Vascular Permeability. As illustrated in Fig. 1E, the vascular leakage of fluorescein isothiocyanate labeled albumin (FITC-albumin) in the ARDS mice was significantly suppressed after uridine treatment. Furthermore, we also evaluated the effect of uridine on CD31 expression in the LPS-induced ARDS mice. As shown in Fig. 1F, uridine treatment regulated CD31 expression in the LPS-induced ARDS model.

Previous study has showed that SDC-1 is one of the main components of the endothelial glycocalyx in pulmonary blood vessels. Therefore, SDC-1 can be used to evaluate damages to the endothelial glycocalyx [9, 10]. The experimental results showed that SDC-1 expression was reduced significantly in LPS-induced ARDS model, indicating that the integrity of the endothelial glycocalyx was damaged. However, uridine could inhibit SDC-1 down-regulation, suggesting that uridine could enhance the integrity of the endothelial glycocalyx (Fig. 1G).

Uridine inhibited ROS production induced by LPS in MLE-12 cells (*in vitro*)

Reactive oxygen species (ROS) are a major risk factor in the onset and progression of oxidative stress. For this reason we studied the effects of uridine on the intracellular ROS level, and our results indicated that uridine could significantly counteract ROS generation (Fig. 2A). Furthermore, the levels of MPO and MDA were obviously increased in MLE-12 cells stimulated with LPS, and uridine treatment significantly decreased MPO and MDA concentrations compared with the LPS group (Fig. 2B). To further investigate the antioxidant effects of uridine, the activity of SOD was detected; it can be seen that the activity of SOD was significantly increased in the uridine treatment group (Fig. 2B). In addition, the relationship between NF-κB activation and inflammation has been demonstrated. Therefore, to explore the effects of uridine on the activation of NF-κB signaling in the ARDS cell model, Western-blots were performed, and the results showed that the phosphorylation levels of p-IκBα and p-NF-κB p65 were down-regulated by uridine treatment (Fig. 2C). Taken together, these results suggest that uridine has antioxidant and anti-inflammatory effects partially via inhibiting ROS generation and blocking the NF-κB signaling pathway.

We further investigated the effect of uridine on the levels of proinflammatory cytokines. MLE-12 cells stimulated with LPS obviously had enhanced concentrations of TNF-α and IL-6 (Fig. 3) compared with the control group. However, uridine (20 μg mL^{-1}) treatment prevented the release of the proinflammatory cytokines (TNF-α and IL-6).

Uridine inhibited MLE-12 apoptosis induced by LPS *in vitro*

LPS treatment could lead to MLE-12 cell apoptosis. To determine whether uridine has an effect on the apoptosis of MLE-12 cells induced by LPS treatment, flow cytometry was conducted. As illustrated in Fig. 4, pre-treatment with uridine significantly inhibited the apoptosis of MLE-12
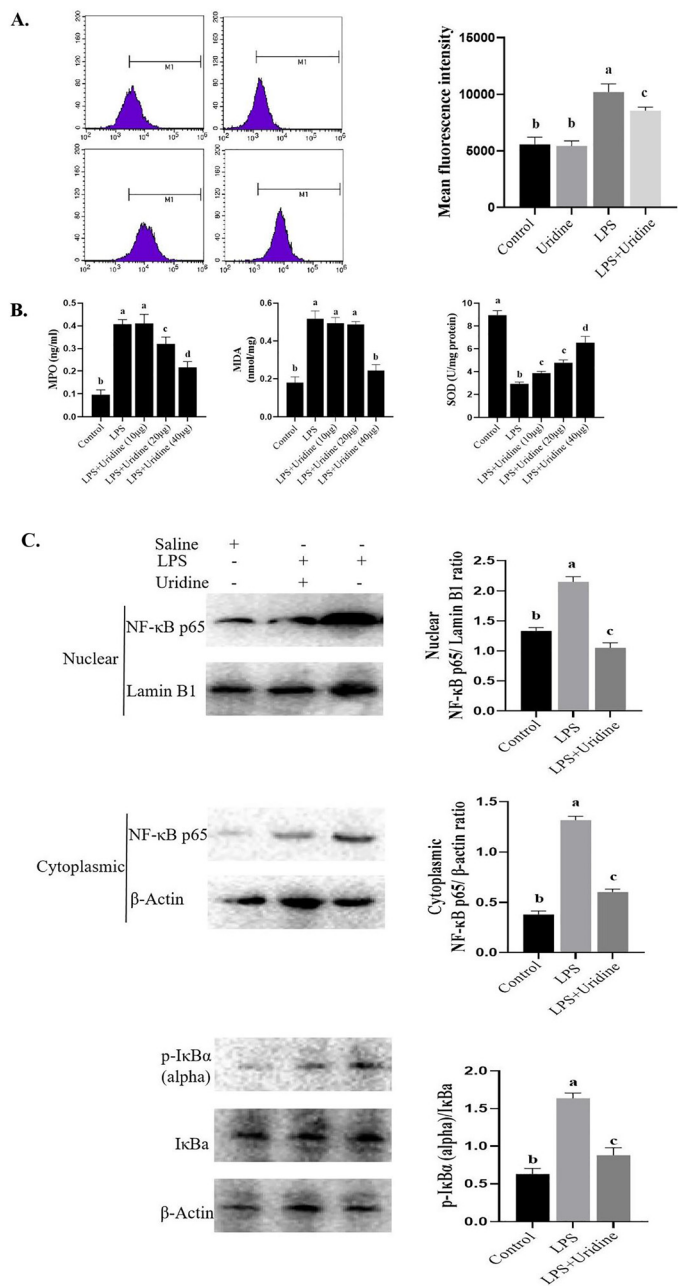
Fig. 2. The effect of uridine on ROS production

A. The cells were pre-treated with uridine (10 μg mL^{-1}) for 3 h before LPS treatment. B. The effect of uridine on oxidative stress markers. C. The effects of uridine on NF-κB signaling in MLE-12 cells evaluated by Western blot analysis. Data are presented as mean ± SD. Different letters indicate significant differences ($P < 0.05$).
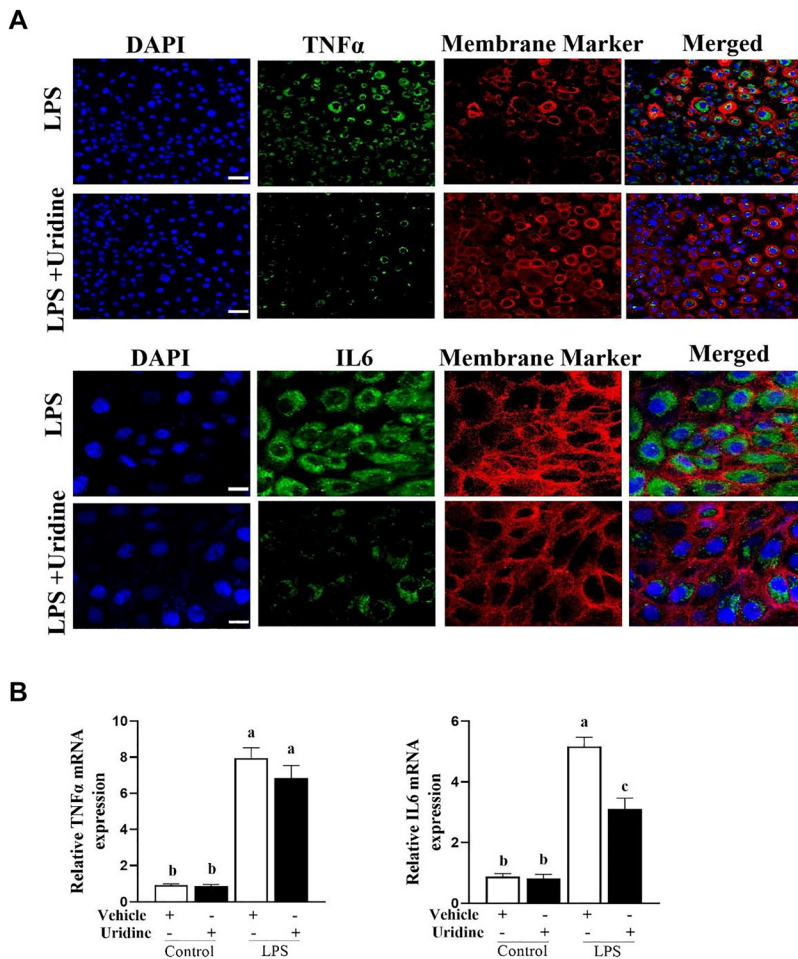
Fig. 3. A. Effects of uridine on IL-6 and TNF-α in lung tissue from LPS-induced ARDS mice. B. Uridine treatment down-regulated the expression of IL 6 and TNFα in the lung tissue. Data are presented as mean ± SD of three independent experiments. Different letters indicate significant differences ($P < 0.05$)

cells. Furthermore, the results from flow cytometry also indicated that uridine could significantly down-regulate the expression of caspase-3 and Bax, and the expression level of Bcl-2 was up-regulated compared to the control group. These findings indicate that uridine plays a protective role in MLE-12's bioactivity.

Uridine inhibited AMPK activation in LPS-induced ARDS mice

It has been reported that AMPK signaling is up-regulated in ARDS mice. As expected, AMPK activation was increased after LPS stimulation in the current study. However, AMPK phosphorylation was significantly down-regulated by uridine treatment, and the phosphorylation levels of JNK, ERK1/2, and p38 were also suppressed by uridine pretreatment (Fig. 5).
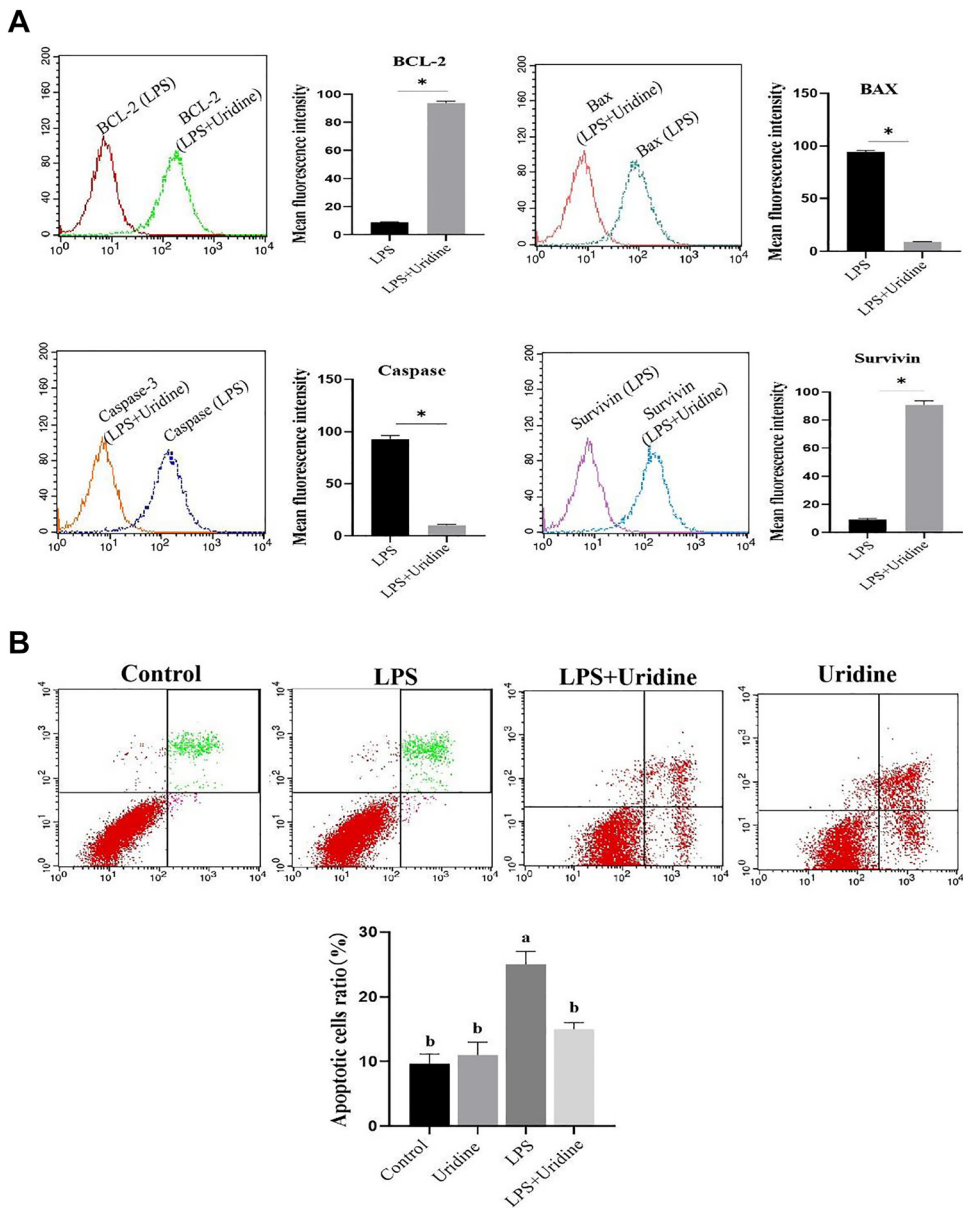
Fig. 4. A. The effect of uridine on the apoptosis of MLE-12 cells induced by LPS treatment. The cells were pre-treated with uridine (10 μg mL^{-1}) for 3 h before LPS treatment. B. The effect of uridine on the expression of caspase-3, Bax and Bcl-2. Data are presented as mean ± SD of three independent experiments. Different letters indicate significant differences ($P < 0.05$)
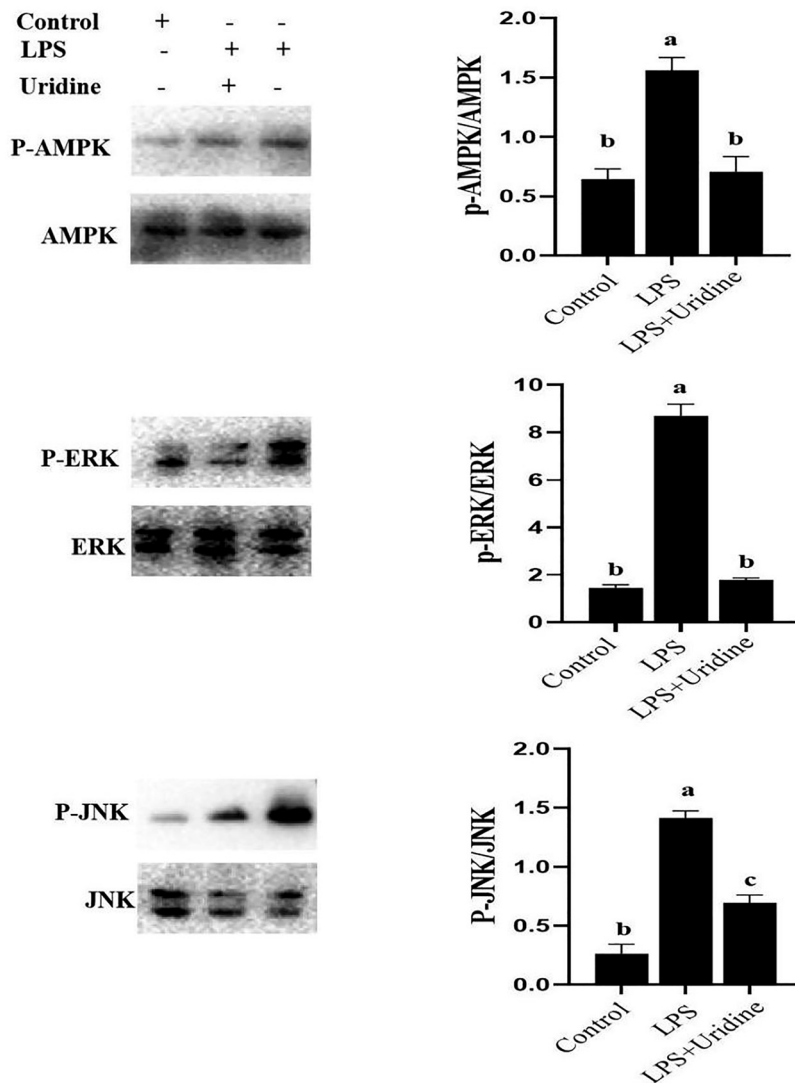
Fig. 5. A. Uridine treatment inhibited the phosphorylation of AMPK, JNK, ERK and p38. Proteins from cells or tissue were extracted using the Tissue Protein Extraction reagent kit according to the manufacturer's instructions. Equal amounts of protein (30 μg) were separated by 10% SDS-PAGE, after which cell protein samples were transferred onto a polyvinylidene difluoride (PVDF) membrane. After blocking in 5% skim milk at 37°C for 120 min, the membranes were incubated with primary antibodies overnight at 4°C, followed by incubating with secondary antibody (1:3000 dilutions) for 60 min on the shaker at RT. After washing, immunoreactive protein bands were detected using an enhanced chemiluminescence system (ECL). Different letters indicate significant differences ($P < 0.05$)
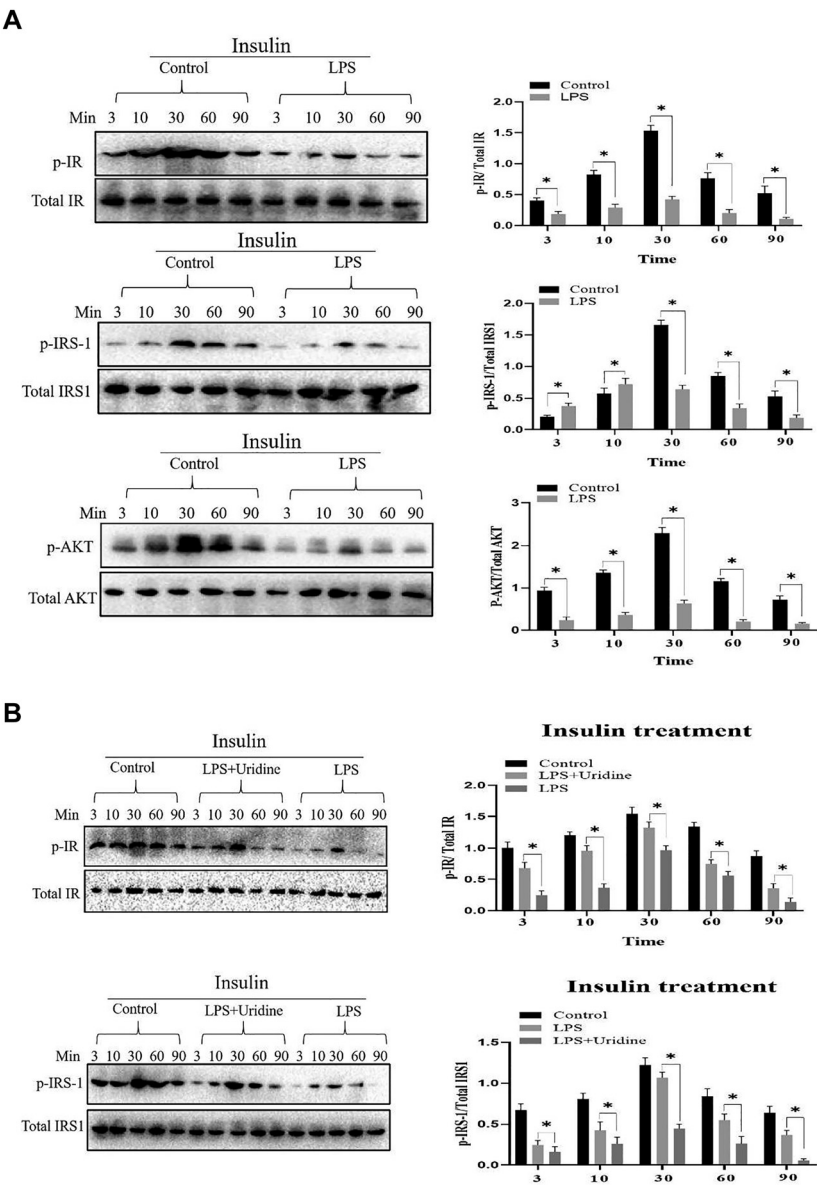
Fig. 6. A. Insulin-mediated signaling in ARDS model mice was down-regulated. Cellular proteins were extracted and quantified using the BCA kit according to the manufacturer's instructions. Equal amounts of protein (30 μg) were separated by 10% SDS-PAGE and then transferred onto a PVDF membrane. After blocking in 5% skim milk at 37°C for 1 h, the membranes were incubated with primary antibodies overnight at 4°C, followed by incubation with a secondary antibody for 60 min on the shaker at RT. After washing, immunoreactive protein bands were observed using the ECL system. B. Uridine pretreatment increased the sensitivity of insulin-mediated signaling. Statistically significant differences ($P < 0.05$) are indicated by asterisks

Insulin-mediated signaling is decreased in ARDS mouse model *in vivo*

In this work we also studied the effect of ARDS on insulin sensitivity. For this, we analyzed the insulin-mediated signaling pathway in ARDS mice, and the results showed that insulin signaling was significantly down-regulated (the liver is one of the most important targets of insulin). In addition, we also analyzed the phosphorylation level of the insulin receptor (IR) in the lungs, and the results also showed that IR activation was significantly down-regulated. These results suggest that insulin sensitivity was significantly down-regulated in the LPS-induced ARDS mice (Fig. 6A).

To investigate the effect of uridine pre-treatment on the insulin/IR-mediated signaling pathway, Western blot analysis was performed, and the results indicated that uridine pre-treatment increased the sensitivity of insulin-mediated signaling (Fig. 6B), demonstrating that uridine could relieve insulin resistance caused by ARDS.

DISCUSSION

Acute Respiratory Distress Syndrome (ARDS) is caused by intrapulmonary and/or extrapulmonary factors [13, 14]. It is a clinical syndrome characterized by intractable hypoxemia. ARDS has attracted much attention due to its high mortality rate. It is generally believed that the excessive activation and recruitment of inflammatory cells in the lung, the activation of a large number of inflammatory factors and effector cells, and the uncontrolled inflammatory response caused by ARDS are the main pathological changes in ARDS [15]. Therefore, inhibiting uncontrolled inflammatory response may be a key approach to treat ARDS. In the current study, we firstly analyzed the effect of uridine on ARDS, and the results showed that uridine could relieve ARDS. On this basis, we further analyzed the effect of ARDS on insulin sensitivity, and our results indicated that ARDS severely affected the sensitivity to insulin, but uridine treatment could improve insulin sensitivity.

A series of studies have shown that the treatment of ARDS by using biologically active molecules is an effective approach. It has been reported that Astilbin could alleviate LPS-induced ARDS by suppressing the MAPK signaling pathway [7]. Chen et al. [16] reported that *Lycium barbarum* polysaccharide (LBP) could protect against LPS-induced ARDS via inhibiting apoptosis and inflammation in pulmonary endothelial cells. In the current study, we first analyzed the effect of uridine on ARDS, and the results showed that uridine could alleviate ARDS. We also found that uridine can significantly alleviate lung damage induced by LPS. In addition, the levels of proinflammatory cytokines (such as TNF-α and IL-6) were evaluated, and the results indicated that TNF-α and IL-6 were significantly decreased in the lung tissue from ARDS mice by uridine treatment. Additionally, the total numbers of cells and neutrophils in BALF were obviously increased compared to the control group. These findings show that uridine can alleviate ARDS. In addition, uridine treatment (physiological concentration) could inhibit intracellular ROS generation and increase SOD activity in the MLE-12 cell model. Furthermore, uridine pretreatment suppressed the expression of active caspase-3 and Bax, and enhanced the expression of Bcl-2.

Next, we further analyzed the underlying mechanism by which uridine alleviates or inhibits ARDS, and our results showed that the NF-κB signaling pathway was significantly inhibited. In addition, it has been reported that MAPK signaling is up-regulated in the ARDS model, and

uridine treatment also decreased AMPK phosphorylation. Furthermore, the phosphorylation levels of JNK, ERK, and p38 were suppressed by uridine treatment. Additionally, accumulating evidence shows that ROS is required for the induction of apoptosis in inflammatory cells [12]. It has been reported that ROS could up-regulate the expression of pro-inflammatory cytokines, and maintaining the oxidant-antioxidant balance is critical in ARDS treatment [12]. Therefore, in the current work we also evaluated the effect of uridine on oxidative stress, and the results showed that the level of oxidative stress was down-regulated by uridine treatment.

In fact, a series of excellent studies from Mironova's team has shown the important biological activity of uridine [17–20]; these authors also found that uridine can protect against LPS-induced inflammation and hypoxia-induced lung damage. One of these studies by Mironova et al. also indicated that the mechanism of the anti-inflammatory action of uridine can be associated with the inhibition of the NF-κB signaling pathway [17]. It was also found that uridine can protect against hypoxia-induced damage to the ultrastructure of the lung tissue [18]. These studies combined with our current work have laid a solid foundation for further exploring the biological activity of uridine.

Next, we studied the effect of ARDS on insulin sensitivity *in vivo*, and the results indicated that insulin signaling was significantly down-regulated in ARDS mice. Furthermore, we found that uridine pretreatment increased the insulin sensitivity. In addition, we also found that the levels of inflammation and oxidative stress were also decreased, which may be a potential molecular mechanism by which uridine could enhance insulin sensitivity.

In conclusion, the present work demonstrates that uridine could protect against LPS-induced ARDS through inhibiting inflammation and oxidative stress (at least partially). More interestingly, we found that ARDS leads to insulin resistance, and uridine treatment can improve insulin sensitivity in the ARDS model. To the best of our knowledge, this is the first study on the effect of uridine on ARDS. Taken together, the current work provides preclinical evidence that uridine can serve as a health food or drug to treat ARDS.

Conflict of interest: The authors declare that they have no conflict of interest.

REFERENCES

1. Ji M, Chen M, Hong X, Chen T, Zhang N. The effect of diabetes on the risk and mortality of acute lung injury/acute respiratory distress syndrome: a meta-analysis. Medicine (Baltimore) 2019; 98(13): e15095. https://doi.org/10.1097/MD.0000000000015095.
2. Chen X, Tang J, Shuai W, Meng J, Feng J, Han Z. Macrophage polarization and its role in the pathogenesis of acute lung injury/acute respiratory distress syndrome. Inflamm Res. 2020; 69(9): 883–95. https://doi.org/10.1007/s00011-020-01378-2.
3. Deshpande R, Zou C. Pseudomonas aeruginosa induced cell death in acute lung injury and acute respiratory distress syndrome. Int J Mol Sci. 2020; 21(15): 5356. https://doi.org/10.3390/ijms21155356.
4. Lew TW, Kwek TK, Tai D, Earnest A, Loo S, Singh K, et al. Acute respiratory distress syndrome in critically ill patients with severe acute respiratory syndrome. JAMA 2003; 290(3): 374–80. https://doi.org/10.1001/jama.290.3.374.

5. Stapleton RD, Wang BM, Hudson LD, Rubenfeld GD, Caldwell ES, Steinberg KP. Causes and timing of death in patients with ARDS. Chest 2005; 128(2): 525–32. https://doi.org/10.1378/chest.128.2.525.

6. Wu C, Chen X, Cai Y, Xia Ja, Zhou X, Xu S, et al. Risk factors associated with acute respiratory distress syndrome and death in patients with coronavirus disease 2019 Pneumonia in Wuhan, China. JAMA Intern Med. 2020; 180(7): 934–43. https://doi.org/10.1001/jamainternmed.2020.0994.

7. Kong G, Huang X, Wang L, Li Y, Sun T, Han S, et al. Astilbin alleviates LPS-induced ARDS by suppressing MAPK signaling pathway and protecting pulmonary endothelial glycocalyx. Int Immunopharmacol. 2016; 36: 51–8. https://doi.org/10.1016/j.intimp.2016.03.039.

8. Hetzel M, Bachem M, Anders D, Trischler G, Faehling M. Different effects of growth factors on proliferation and matrix production of normal and fibrotic human lung fibroblasts. Lung 2005; 183(4): 225–37. https://doi.org/10.1007/s00408-004-2534-z.

9. Liu XY, Xu HX, Li JK, Zhang D, Ma XH, Huang LN, et al. Neferine protects endothelial glycocalyx via mitochondrial ROS in lipopolysaccharide-induced acute respiratory distress syndrome. Front Physiol. 2018; 9: 102. https://doi.org/10.3389/fphys.2018.00102.

10. Ma X, Liu X, Feng J, Zhang D, Huang L, Li D, et al. Fraxin alleviates LPS-induced ARDS by downregulating inflammatory responses and oxidative damages and reducing pulmonary vascular permeability. Inflammation. 2019; 42(5): 1901–12. https://doi.org/10.1007/s10753-019-01052-8.

11. Jeengar MK, Thummuri D, Magnusson M, Naidu VGM, Uppugunduri S. Uridine ameliorates dextran Sulfate Sodium (DSS)-Induced colitis in mice. Sci Rep. 2017; 7(1): 3924. https://doi.org/10.1038/s41598-017-04041-9.

12. Simon HU, Haj-Yehia A, Levi-Schaffer F. Role of reactive oxygen species (ROS) in apoptosis induction. Apoptosis 2000; 5(5): 415–8. https://doi.org/10.1023/a:1009616228304.

13. Pan L, Yao DC, Yu YZ, Li SJ, Chen BJ, Hu GH, et al. Necrostatin-1 protects against oleic acid-induced acute respiratory distress syndrome in rats. Biochem Biophys Res Commun. 2016; 478(4): 1602–8. https://doi.org/10.1016/j.bbrc.2016.08.163.

14. Tang PS, Mura M, Seth R, Liu M. Acute lung injury and cell death: how many ways can cells die? Am J Physiol Lung Cell Mol Physiol. 2008; 294(4): L632–41. https://doi.org/10.1152/ajplung.00262.2007.

15. Kitamura Y, Hashimoto S, Mizuta N, Kobayashi A, Kooguchi K, Fujiwara I, et al. Fas/FasL-dependent apoptosis of alveolar cells after lipopolysaccharide-induced lung injury in mice. Am J Respir Crit Care Med. 2001; 163(3 Pt 1): 762–9. https://doi.org/10.1164/ajrccm.163.3.2003065.

16. Chen L, Li W, Qi D, Wang D. Lycium barbarum polysaccharide protects against LPS-induced ARDS by inhibiting apoptosis, oxidative stress, and inflammation in pulmonary endothelial cells. Free Radic Res. 2018; 52(4): 480–90. https://doi.org/10.1080/10715762.2018.1447105.

17. Mironova GD, Khrenov MO, Talanov EY, Glushkova OV, Parfenyuk SB, Novoselova TV, et al. The role of mitochondrial KATP channel in anti-inflammatory effects of uridine in endotoxemic mice. Arch Biochem Biophys. 2018; 654: 70–6. https://doi.org/10.1016/j.abb.2018.07.006.

18. Rozova EV, Mankovskaya IN, Belosludtseva NV, Khmil NV, Mironova GD. Uridine as a protector against hypoxia-induced lung injury. Sci Rep. 2019; 9(1): 9418. https://doi.org/10.1038/s41598-019-45979-2.

19. Krylova IB, Selina EN, Bulion VV, Rodionova OM, Evdokimova NR, Belosludtseva NV, et al. Uridine treatment prevents myocardial injury in rat models of acute ischemia and ischemia/reperfusion by activating the mitochondrial ATP-dependent potassium channel. Sci Rep. 2021; 11(1): 16999. https://doi.org/10.1038/s41598-021-96562-7.

20. Krylova IB, Kachaeva EV, Rodionova OM, Negoda AE, Evdokimova NR, Balina MI, et al. The cardioprotective effect of uridine and uridine-5′-monophosphate: the role of the mitochondrial ATP-dependent potassium channel. Exp Gerontol. 2006; 41(7): 697–703. https://doi.org/10.1016/j.exger.2006.03.005.